Effect of NaCl and KCl on Phosphatidylcholine and Phosphatidylethanolamine Lipid Membranes: Insight from Atomic-Scale Simulations for Understanding Salt-Induced Effects in the Plasma Membrane

Andrey A. Gurtovenko*,† and Ilpo Vattulainen‡,§,||

Computational Biophysics Laboratory, Institute of Pharmaceutical Innovation, Bradford, West Yorkshire BD7 1DP, UK, Institute of Physics, Tampere University of Technology, P.O. Box 692, FI−33101 Tampere, Finland, Helsinki University of Technology, P.O. Box 1100, FI−02015 HUT, Finland, and MEMPHYS − Center for Biomembrane Physics, University of Southern Denmark, Odense, Denmark

Received: June 29, 2007; In Final Form: November 19, 2007

To gain a better understanding of how monovalent salt under physiological conditions affects plasma membranes, we have performed 200 ns atomic-scale molecular dynamics simulations of phosphatidylcholine (PC) and phosphatidylethanolamine (PE) lipid bilayers. These two systems provide representative models for the outer and inner leaflets of the plasma membrane, respectively. The implications of cation−lipid interactions in these lipid systems have been considered in two different aqueous salt solutions, namely NaCl and KCl, and the sensitivity of the results on the details of interactions used for ions is determined by repeating the simulations with two distinctly different force fields. We demonstrate that the main effect of monovalent salt on a phospholipid membrane is determined by cations binding to the carbonyl region of a membrane, while chloride anions mostly stay in the water phase. It turns out that the strength and character of the cation−lipid interactions are quite different for different types of lipids and cations. PC membranes and Na^+ ions demonstrate strongest interactions, leading to notable membrane compression. This finding was confirmed by both force fields (Gromacs and Charmm) employed for the ions. The binding of potassium ions to PC membranes (and the overall effect of KCl), in turn, was found to be much weaker mainly due to the larger size of a K^+ ion compared to Na^+. Furthermore, the effect of KCl on PC membranes was found to be force-field sensitive: The binding of a potassium ion was not observed at all in simulations performed with the Gromacs force-field, which seems to exaggerate the size of a K^+ ion. As far as PE lipid bilayers are concerned, they are found to be influenced by monovalent salt to a significantly lesser extent compared to PC bilayers, which is a direct consequence of the ability of PE lipids to form both intra- and intermolecular hydrogen bonds and hence to adopt a more densely packed bilayer structure. Whereas for NaCl we observed weak binding of Na^+ cations to the PE lipid−water interface, in the case of KCl we witnessed almost complete lack of cation binding. Overall, our findings indicate that monovalent salt ions affect lipids in the inner and outer leaflets of plasma cell membranes in substantially different ways.

I. Introduction

A lipid bilayer is generally considered as a structural matrix for molecules such as proteins and cholesterol, which are embedded in the lipid bilayer. Together, they form complex cell membrane structures.[1] The cell membranes are involved in a variety of cellular functions, for which reason their composition and distribution are regulated in many ways. The asymmetric distribution of lipids across a membrane provides one means for this purpose. This is highlighted by the distribution of lipids in the plasma membrane of eukaryotic cells, where the lipid composition in the outer and inner leaflets of the membrane differs substantially from each other. In the outer leaflet, the most abundant class of lipids are phosphatidylcholines (PCs), while the inner leaflet is mostly comprised of phosphatidylethanolamines (PEs).[2]

Under physiological conditions, lipids in biological membranes interact with a solution of salt ions, whose detailed composition depends on the membrane region in question. Considering the biological relevance of salt ions, the most important ones include Na^+, K^+, Cl^-, Ca^{2+}, and Mg^{2+}. The role of divalent Ca^{2+} is particularly important, e.g., in mitochondrial membranes, whereas monovalent ions such as Na^+ and K^- are important in modulating the properties of the plasma membrane, for example.[3−5] Recent experimental studies[6−9] have demonstrated that monovalent cations such as sodium can have a significant impact on lipid membranes: Ion binding enhances lipid−lipid interactions and leads to a compression of the membrane. The impact of potassium ions on phospholipid membranes seems to be weaker compared to sodium ions.[5,9]

As computational modeling has become an irreplaceable tool for finding molecular-level information of complex many-component membrane systems,[10] it is expected that simulations can also provide a great deal of insight into the salt-induced effects on lipid membranes. The main obstacle in such studies is related to rather long time scales associated with the binding of ions to lipid membranes. Consequently, the first realistic atomic-scale simulations of membranes under the influence of salt have been performed only rather recently. The majority of studies have by far dealt with effects of salt on zwitterionic

* Corresponding author e-mail: A.Gurtovenko@bradford.ac.uk.
† University of Bradford.
‡ Tampere University of Technology.
§ Helsinki University of Technology.
|| University of Southern Denmark.

10.1021/jp0750708 CCC: $40.75
Published on Web 01/29/2008

(neutral) lipid bilayers,[6,11−16] though an increasing number of studies have also gauged the effects of (counter)ions on anionic[17−20] and cationic[21,22] lipid membranes.

Considering the plasma membrane of eukaryotic cells, the computational studies that have been carried out by far have focused on the effect of monovalent[6,12,14,15] (NaCl) and divalent[11] ($CaCl_2$) salts on bilayers comprised of zwitterionic PCs. This setup essentially corresponds to the *outer* leaflet of the plasma membrane. The studies have provided compelling evidence that cations are able to penetrate deep into a membrane up to the carbonyl region and form tight complexes with lipid molecules.[6,11,12,15] Characteristic times required for ion binding to occur were found to be ∼30 ns for sodium ions[6] and as long as 100 ns for divalent calcium.[11] The binding of cations has been found to have a significant impact on the structural and dynamical properties of PC membranes: It leads to a drop in the area per lipid accompanied by an enhanced ordering of lipid acyl chains and the slowing down of lateral diffusion in the membrane plane.[6,11,12,15]

The understanding of salt-induced effects on plasma membranes is largely incomplete, however. This is due to the lack of studies on the effect of salt ions on phosphatidylethanolamine (PE) lipid membranes. The PE lipids are abundant in the *inner* leaflet of plasma membranes and their interactions with ions can be highly relevant for understanding membrane properties. This issue is especially relevant for interactions between a PE leaflet and potassium ions, since the inner leaflet of the plasma membrane faces a major molar concentration of potassium ions. This is in contrast to the outer (PC) leaflet, which in turn is influenced by a substantial concentration of sodium ions.

To extend the understanding of salt-induced effects on lipid membranes under physiological conditions, in this work we use extensive atomic-scale molecular dynamics (MD) simulations to characterize the influence of NaCl and KCl salts on PC and PE lipid membranes in a systematic fashion. We demonstrate that the effect of monovalent salt strongly depends on the type of lipids and cations: Interactions of sodium ions with the phospholipid−water interface are considerably stronger than those of potassium ions, and PC membranes are influenced by monovalent salt to a significantly larger extent than PE bilayers. Our recent study provided a preliminary view on the interactions of KCl with PC membranes.[23] Furthermore, as the development of accurate ion force fields has turned out to be a rather challenging task,[24] we discuss this matter by considering the sensitivity of simulation results to a choice of the force-field employed for ions.

II. Materials and Methods

We have performed atomic-scale molecular dynamics simulations of single-component lipid bilayers comprised of zwitterionic palmitoyl-oleoyl-phosphatidylcholine (POPC) and palmitoyl-oleoyl-phosphatidylethanolamine (POPE) lipids in aqueous solution with either NaCl or KCl salt. A typical simulation system consists of 128 lipids, about 5000 water molecules, 20 cations, and 20 anions; the corresponding salt concentration is ∼0.2 M.

Force-field parameters for POPC lipids were taken from the united atom force-field of Berger et al.;[25] To make a self-consistent systematic comparison of the properties of POPC and POPE lipid bilayers, we chose to use the same set of parameters for POPE lipids with the exception of the head group region: PE head groups were described following the POPE model of Tieleman and Berendsen.[26] Recently, we have used this force-field for MD simulation studies of asymmetric lipid membranes built from PC and PE leaflets.[27] Water was modeled using the simple point charge (SPC) model.[28] For sodium, potassium, and chloride ions were employed two different sets of parameters. The first set was originally developed in ref 29 and is supplied within the GROMACS force-field.[30] The second set is based on parameters developed by Roux and Beglov[31] and incorporated into the Charmm force-field (these are available online at: http://thallium.bsd.uchicago.edu/RouxLab/downloads/charmm/parameters/ions.dat). The ion parameters employed in this study are summarized in Table 1.

TABLE 1: Lennard-Jones Parameters of Ions

ions	σ (nm)[a]	ϵ (kJ/mol)[a]
Na^+	0.25752 (0.24299)	0.061774 (0.19629)
K^+	0.64541 (0.31426)	0.56651×10^{-4} (0.364001)
Cl^-	0.44480 (0.40447)	0.44559 (0.62760)

[a] Presented are parameters for the Gromacs force-field (Charmm parameters are shown in brackets).

We note that the Charmm force-field parameters for ions were developed in conjunction with the TIP3P water model. As mentioned above, in this study we use the SPC water model as it is dictated by the choice of the force-field for phospholipids. The binding of ions to lipid carbonyl oxygens is accompanied by the loss of water molecules from the first hydration shell of ions. Since the hydration of ions is slightly different when the SPC and TIP3P water models are employed, one might expect that the use of a particular water model could affect ion binding to the membrane surface. However, this effect (if present at all) should be rather weak as the binding is a stochastic process: An ion driven by thermal fluctuations can appear occasionally in the vicinity of the water−lipid interface and eventually bind to a lipid, provided that the simulation is extended to long enough times. As an illustration of this matter, one can consider the binding of divalent Ca ions to a phospholipid membrane. The electrostatic attraction between water molecules with divalent cations is considerably stronger than with their monovalent counterparts; this, however, leads only to the slowing down of the ion binding.[11] Thus, the choice of a water model should hardly affect the binding of salt ions to lipid carbonyl oxygens, and therefore the main findings of the paper. Further, the use of the Charmm force-field for ions, and the comparison of related results with those obtained by the Gromacs force-field, provides insight for the sensitivity of membrane properties on the details of the ion force field.

The Lennard-Jones interactions were cut off at 1 nm. For the electrostatic interactions, we used the particle-mesh Ewald method[32,33] which has been shown to perform very well in membrane simulations.[34−36] Simulations were performed in the *NpT* ensemble at the physiological temperature ($T = 310$ K) and at a pressure set to 1 bar; temperature and pressure were kept constant by the Berendsen scheme.[37] The time step used in all simulations was 2 fs.

Overall, eight different bilayer systems with salt were considered: Two different lipid bilayers (POPC and POPE) in aqueous solution with two different salts (NaCl and KCl) modeled by two distinct sets of parameters for ions (Gromacs and Charmm). Every bilayer system was simulated for 200 ns. As a reference, two 100 ns long MD trajectories of salt-free POPC and POPE lipid bilayers were taken from ref 27. The total simulated time amounted to 1.6 microseconds. Equilibration of the systems is discussed below. All simulations were performed using the GROMACS suite.[30]

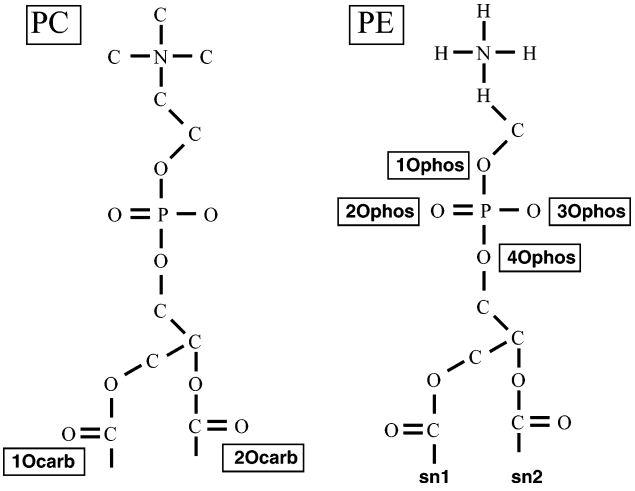

Figure 1. Chemical structure of the head group region of phosphatidylcholine, PC (left), and phosphatidylethanolamine, PE (right).

III. Results and Discussion

A. Effect of Monovalent Salt on POPC Membranes. We start by considering the effects of monovalent salt on POPC lipid membranes, whose head group region is sketched in Figure 1 (left). In Table 2, we have summarized several structural characteristics computed for all bilayer systems we have studied.

Salt-Free POPC. For a salt-free POPC bilayer at 310 K the area per lipid was found to be 0.652 ± 0.002 nm^2 (the area was averaged over the last 70 ns out of 100 ns trajectory). On the experimental side, values of 0.66 nm^2 ($T = 310$ K),[38] 0.65 nm^2 ($T = 298$ K),[39] 0.64 nm^2 ($T = 298$ K),[40] and 0.63 nm^2 ($T = 297$ K)[41] have been reported for the area per lipid for POPC bilayers. Therefore, our value for the area per lipid is in good agreement with available experimental data (as well as with previous MD studies[6,42,43]), validating thereby the molecular model employed in this study. Furthermore, the average angle between the P−N vector (from phosphorus to nitrogen in the head group) and the outward bilayer normal for a POPC bilayer was found to be around 78 degrees, in agreement with previous studies.[27] To characterize the dynamic properties of phospholipid bilayers, we focused on the lateral mobility of lipid molecules. The lateral diffusion coefficient D_L was evaluated as $D_L = \lim_{t\to\infty}(1/4t)\langle[\vec{r}(t) - \vec{r}(0)]^2\rangle$, i.e., from the slope of the mean-square displacement $\langle[\vec{r}(t) - \vec{r}(0)]^2\rangle$ of lipids' centers of mass in the bilayer plane. To improve accuracy, the effects of the motion of the centers of mass of two monolayers relative to each other as well as barostat effects were excluded. Each 100 ns production run was splitted into four pieces; for every piece of 25 ns we computed the mean-square displacement $\langle[\vec{r}(t) - \vec{r}(0)]^2\rangle$ up to $t = 12.5$ ns. The slope of $\langle[\vec{r}(t) - \vec{r}(0)]^2\rangle$ was then evaluated within a time window from 4 to 8 ns. The diffusion coefficient D_L was calculated separately for every piece of trajectory, providing thereby an estimation for the error margin.[6,15] The lateral diffusion coefficients D_L for all bilayer systems studied in the paper are summarized in Table 3. In particular, for the diffusion coefficient of a salt-free POPC membrane, we found $D_L = (5.68 \pm 0.82) \times 10^{-8}$ cm^2/s in reasonable agreement with previous studies.[6]

POPC Under the Influence of NaCl. Addition of NaCl drastically changes the structural properties of a POPC lipid bilayer through the binding of cations to the lipid−water interface. Previous MD studies clearly demonstrated that ion binding is a rather slow process, which emphasizes the fact that system equilibration is one of the central issues in simulations of lipid bilayers with salt.[6,11,15] Hence, in simulations with salt there is reason to monitor equilibration not only through the time evolution of the area per lipid but also through the time development of coordination numbers of cations with some principal lipid oxygens. Similar to previous studies,[6,11,15] here we consider the coordination of cations with lipid carbonyl and water oxygens. For that purpose, the radial distribution functions (RDFs) of cations and the oxygens were calculated and the radii of the first hydration shells were extracted. Coordination numbers were then computed by counting the number of oxygen atoms in the first hydration shell of a cation.

In Figure 2 we show the time evolution of coordination numbers N_C of Na^+ ions with POPC carbonyl and water oxygens. The binding of a sodium ion to the carbonyl region of a PC membrane is clearly seen through increasing coordination of a sodium ion with the carbonyl oxygens of POPC lipids (atoms 1Ocarb and 2Ocarb in Figure 1), accompanied by a significant loss of water oxygens from the ion's first coordination shell.

Figure 2 shows that this process can take up to 80−90 ns. We note that for the bilayer system in which Gromacs force-field parameters are used for ions (Figure 2 (top)) the coordination numbers do not look completely stabilized even after 200 ns; their deviations from the equilibrium state are rather small, though. Other computational studies[6,11,15,23] that employed the same force-field for lipids and ions showed, however, complete equilibration within 30−40 ns, so that the deviation observed in the present work can be considered as a fluctuation. Therefore, all structural characteristics presented in this work have been calculated over the last 100 ns (out of 200 ns long MD trajectories).

The tight binding of sodium ions to the carbonyl oxygens of POPC lipids affects the structural properties of a membrane. In particular, it leads to a considerable compression of the membrane coupled to an enhanced ordering of hydrocarbon lipid chains. Another important structural characteristic of zwitterionic phospholipid bilayers is the orientation of lipid head groups with respect to the outward bilayer normal. It is of particular interest since the orientation of the dipole moment in the lipid head group contributes to the electrostatic potential across a lipid monolayer. Complexation of lipids with cations leads to a remarkable reorientation of PC head groups toward the water phase, see Table 2. The cation−lipid complexation is also responsible for a dramatic decrease in the lateral mobility of lipids seen via up to ∼50% drop in the diffusion coefficient D_L of a POPC bilayer with NaCl salt, see Table 3.

The above findings are in good agreement with experimental data[6−9] and with previously reported computational results.[6,12,15] It is, however, very instructive to consider the sensitivity of the results to a force-field employed for modeling salt ions. For doing that we performed simulations for all bilayer systems using two distinct sets of ion parameters, Gromacs and Charmm (results related to the Charmm force-field are shown in brackets throughout Tables 2 and 3). As one can see, both sets of parameters give very similar results regarding the area per lipid (0.604 nm^2 for Gromacs and 0.608 nm^2 for Charmm), the fraction of cations $\chi_{\text{bound}}^{(\text{cations})}$ adsorbed on a membrane (0.87 vs 0.85), and the lateral diffusion coefficients D_L (3.11×10^{-8} cm^2/s vs 3.20×10^{-8} cm^2/s). However, the character of ion binding was found to be rather different: As seen from Figure 2, sodium ions in the Gromacs force field description bind to lipid head groups considerably stronger than in the case where the Charmm force field parameters are being used. On average, a sodium

TABLE 2: Summary of MD Simulations of Phospholipid Membranes with Monovalent Salt

	lipids	salt[a]	$\langle A \rangle$ (nm^2)[b]	$\langle N_{coord}^{(cations)} \rangle$ [c]	$\langle \chi_{bound}^{(cations)} \rangle$ [d]	$\langle N_{coord}^{(anions)} \rangle$ [c]	$\langle \chi_{bound}^{(anions)} \rangle$ [d]	$\langle \phi_{PN} \rangle$ (deg)[e]
1	POPC		0.652					77.9
2	POPC	NaCl	0.604 (0.608)	3.09 (2.14)	0.87 (0.85)	1.30 (1.22)	0.30 (0.25)	71.3 (69.6)
3	POPC	KCl	0.648 (0.639)	1.17 (1.88)	0.07 (0.37)	1.15 (1.13)	0.17 (0.17)	77.3 (74.2)
4	POPE		0.519					92.8
5	POPE	NaCl	0.509 (0.511)	2.99 (2.38)	0.24 (0.34)	1.36 (1.11)	0.16 (0.15)	89.9 (88.6)
6	POPE	KCl	0.511 (0.509)	0.16 (1.66)	0.01 (0.06)	1.20 (0.94)	0.11 (0.08)	93.1 (93.6)

[a] Two force-fields, Gromacs and Charmm, were employed for salt ions. Shown in brackets are values corresponding to Charmm ion parameters. [b] The area per lipid, $\langle A \rangle$; errors for $\langle A \rangle$ were estimated to be $\sim$0.002 nm^2. The errors throughout the study were computed as standard errors of mean by splitting a trajectory into 10 ns pieces. [c] Coordination numbers of cations with lipid carbonyl oxygens, $N_{coord}^{(cations)}$, and of anions with nitrogen atoms of phospholipids, $N_{coord}^{(anions)}$. Errors for $N_{coord}^{(cations)}$ were found to be in the range from 0.03 to 0.09; errors for $N_{coord}^{(anions)}$ were less than 0.03. [d] Fractions of cations and anions, $\chi_{bound}^{(cations)}$ and $\chi_{bound}^{(anions)}$, bound to carbonyl oxygens and nitrogens of phospholipid molecules, respectively. A cation (anion) was considered to be bound to the lipid−water interface if it has a carbonyl oxygen (nitrogen) in its first coordination shell. Errors for fractions of sodium and chloride ions did not exceed 5%, whereas errors for fractions of potassium ions were in the range from 3.5 to 14.5%. [e] The average angle between the P−N vector of a lipid head group and the outward bilayer normal; errors were found to be less than 0.3 degrees.

TABLE 3: Lateral Diffusion Coefficients D_L of POPC and POPE Membranes

	lipids	salt	D_L (10^{-8}cm^2/s)[a]
1	POPC		5.68 ± 0.82
2	POPC	NaCl	3.11 ± 0.47 (3.20 ± 0.76)
3	POPC	KCl	6.36 ± 1.64 (4.97 ± 0.97)
4	POPE		1.16 ± 0.30
5	POPE	NaCl	0.98 ± 0.20 (1.01 ± 0.27)
6	POPE	KCl	0.71 ± 0.18 (0.84 ± 0.26)

[a] Two force-fields, Gromacs and Charmm, were employed for salt ions. Shown in brackets are values corresponding to Charmm ion parameters. The errors for D_L were computed as standard deviations.

ion binds to 3.09 and 2.14 POPC lipids for Gromacs and Charmm descriptions, respectively (see Table 2). We note that these coordination numbers reflect the actual binding of Na^+ ions to the carbonyl oxygens as the averaging was performed only over ions which have lipid carbonyl oxygens in the first coordination shell; in contrast, the coordination numbers N_C shown in Figure 2 were averaged over all cations in the system.

The somewhat weaker binding of Na^+ ions in Charmm can also be visualized through the component-wise density profiles of various constituents of the system, summarized in Figure 3 (for clarity's sake, the density profiles were normalized by their maximal values). With Gromacs parameters the density profile of Na^+ ions exactly coincides with the profile of lipid carbonyl oxygens, indicating tight complexation. In simulations with the Charmm force-field for ions, the peak of the Na^+ density profile is notably shifted toward phosphate groups, see Figure 3, which suggests weaker binding of sodium ions to the carbonyl oxygens. As a result, in this case sodium ions are closer to the water−lipid interface as compared to the situation seen with Gromacs parameters, and thus Na^+ ions in simulations with Charmm parameters are able to push choline groups somewhat further toward the aqueous phase. The latter is confirmed by the stronger reorientation of head group PC vectors in simulations with Charmm parameters, see Table 2.

The origin of the different character of sodium binding for the two ionic parameter sets is expected to lie in the slightly different sizes of Na^+ ions in Gromacs and Charmm force-fields, see Table 1. The somewhat larger Na^+ ions given by Gromacs parameters are likely able to accommodate more carbonyl oxygens in their first coordination shells compared to simulations performed with the Charmm force-field for ions. It has to be also noted that chloride ions stay mainly in the water phase and bind only very weakly to the interface through transient

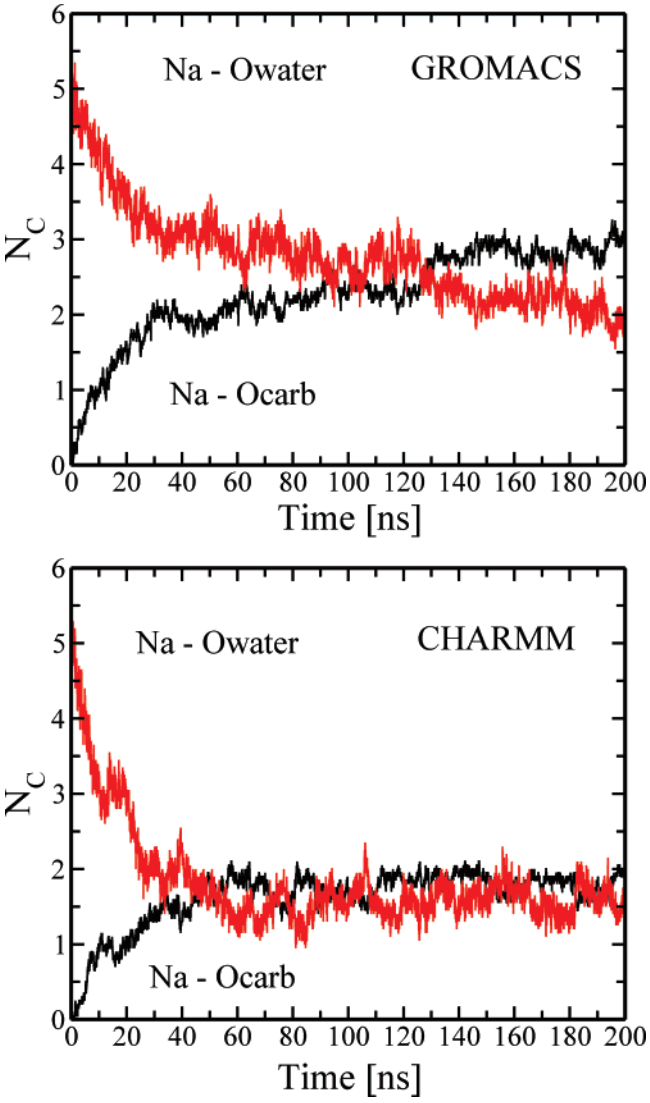

Figure 2. Time evolution of coordination numbers N_C of sodium ions with lipid carbonyl and water oxygens for POPC membranes. Shown are results for Gromacs (top) and Charmm (bottom) force-field parameters used for ions.

coordination with choline groups, see Figure 3 and Table 2; no significant differences were observed for the two sets of ion parameters.

POPC Under the Influence of KCl. Now we turn to the discussion of how KCl affects POPC lipid membranes. It turns out that the effects of the binding of potassium ions to a PC

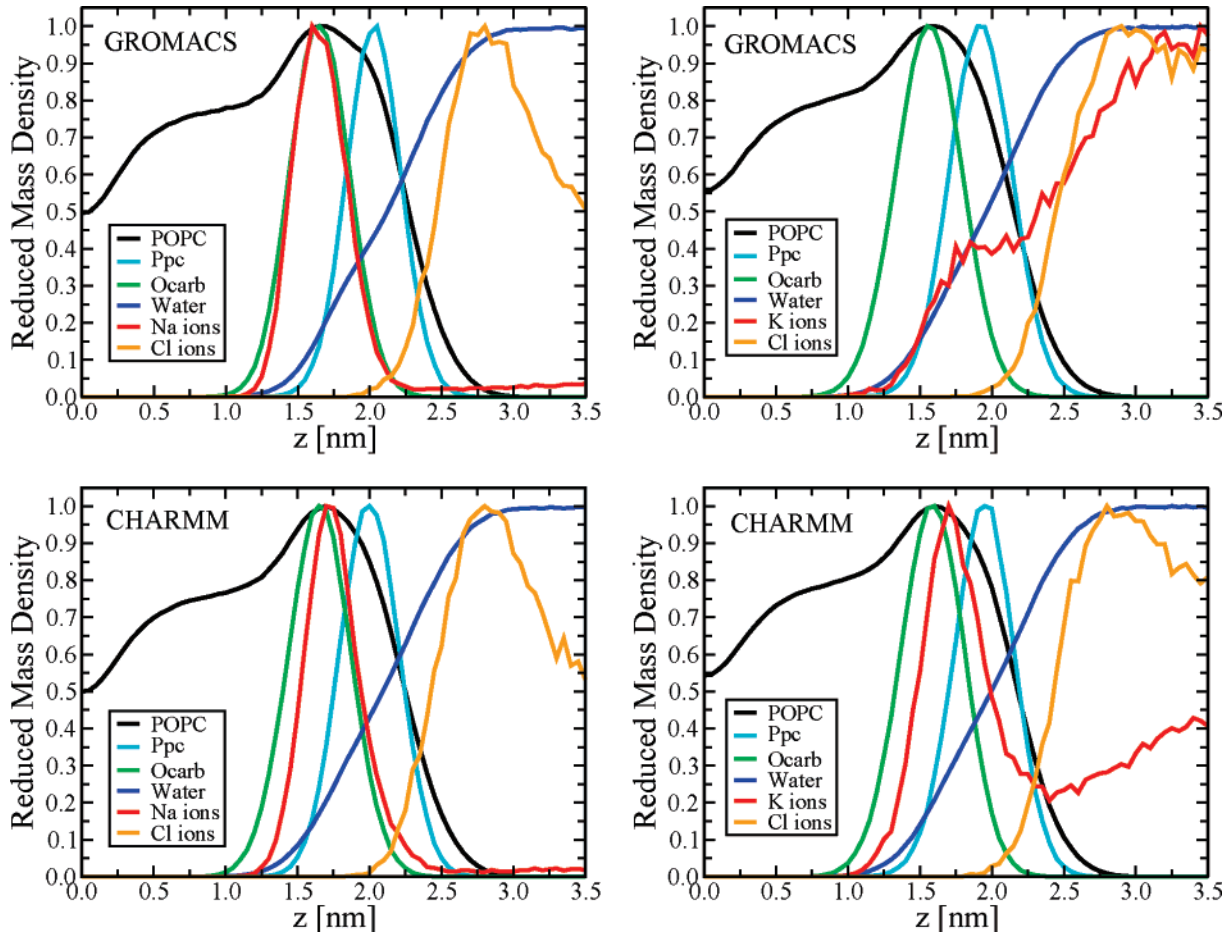

Figure 3. Component-wise density profiles (scaled by the maximal value of each component) as a function of the distance z from the bilayer center ($z = 0$). Shown are results for POPC bilayers with NaCl (left) and KCl (right), salt ions being described by Gromacs (top) and Charmm (bottom) force-fields. All density profiles were averaged over two leaflets.

bilayer are quite different for the two parameter sets employed for the ions. In the case of the Gromacs force-field, the binding of potassium ions is almost fully absent, as most of K^+ ions prefer to be located in the aqueous phase, see Figures 3 and 4. As a consequence, the area per lipid, the average head group orientation, and the lateral lipid mobility remain almost unchanged in the POPC bilayer system when the concentration of KCl is increased from 0 to 0.2 M, see Tables 2 and 3.

The situation is opposite for simulations where the Charmm force field is used for ions: Potassium ions do bind to the lipid−water interface, although to a significantly lesser extent compared to sodium ions, see Figures 3 and 4. As a result, one can witness a minor but noticeable effect of KCl on a POPC membrane, manifested as a rather small compression of the membrane and reorientation of PC head groups as shown in Table 2 and as a small drop in the lateral diffusion coefficient, see Table 3 (also note large error margins for D_L). Such a notable contrast in membrane properties due to the two different force-field parameter sets for K^+ ions can directly be associated with a large difference in the Lennard-Jones parameters of Gromacs and Charmm force-fields. The Lennard-Jones diameter of a K^+ ion in the Gromacs force-field is more than *two times* larger than that in the Charmm force-field (see the parameter σ in Table 1). When compared with the corresponding diameter of a Na^+ ion, the Gromacs force-field for potassium and sodium ions seems to exaggerate the size difference of these ions (>100%), whereas their Pauling ionic radii differ by just 35%, see, e.g., ref 5. Furthermore, the Gromacs value for σ of a K^+ ion employed in this study is much larger than those used in other studies;[31,44−46] Additionally, a very small value of ϵ makes a K^+ ion in the Gromacs force field a hard (large) sphere. For comparison, the value of σ for a potassium ion in the Charmm force field is larger than that for a sodium ion by only ∼30%. On these grounds, it is likely that the Charmm parameter set provides a more realistic description for KCl.

Overall, when the effects of KCl and NaCl are compared with one another, a considerably weaker effect of KCl on POPC membranes is mainly related to the difference in the size of these two cations. A sodium ion, being smaller than a potassium ion, has a larger surface charge and a more ordered first hydration shell, and, therefore, is able to attract water and lipid carbonyl oxygens more strongly. Indeed, the average fractions of cations $\chi_{bound}^{(cations)}$ condensed on the membrane surface are found to be 0.85 for Na^+ ions versus 0.37 for K^+ ions (see Table 2 for simulations with Charmm), so that the binding of sodium ions is much stronger than the binding of potassium ions. Interestingly, the fraction of chloride ions $\chi_{bound}^{(anions)}$ near the membrane surface is notably larger for the POPC system with NaCl than for the bilayer with KCl, see Table 2. This can be explained by the fact that Cl^- ions compete for the lipid−water interface with K^+ ions, while this is not the case for POPC bilayers with NaCl as most sodium ions in this case are located deep in the interface. The effect should vanish with increasing salt concentration. Overall, the above differences in lipid complexation with Na^+ and K^+ ions should hold for any force fields employed for ions as long as the Lennard-Jones diameter of a sodium ion is smaller than that of a potassium ion. The

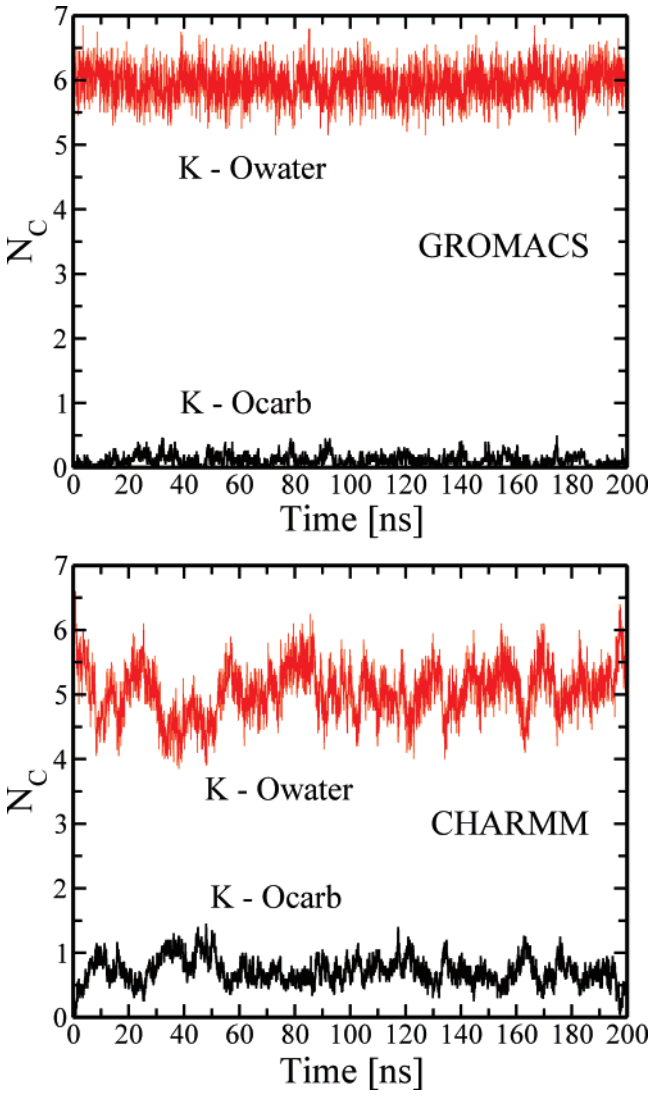

Figure 4. Time evolution of coordination numbers N_C of potassium ions with lipid carbonyl and water oxygens for POPC membranes. Shown are results for Gromacs (top) and Charmm (bottom) force-field parameters used for ions.

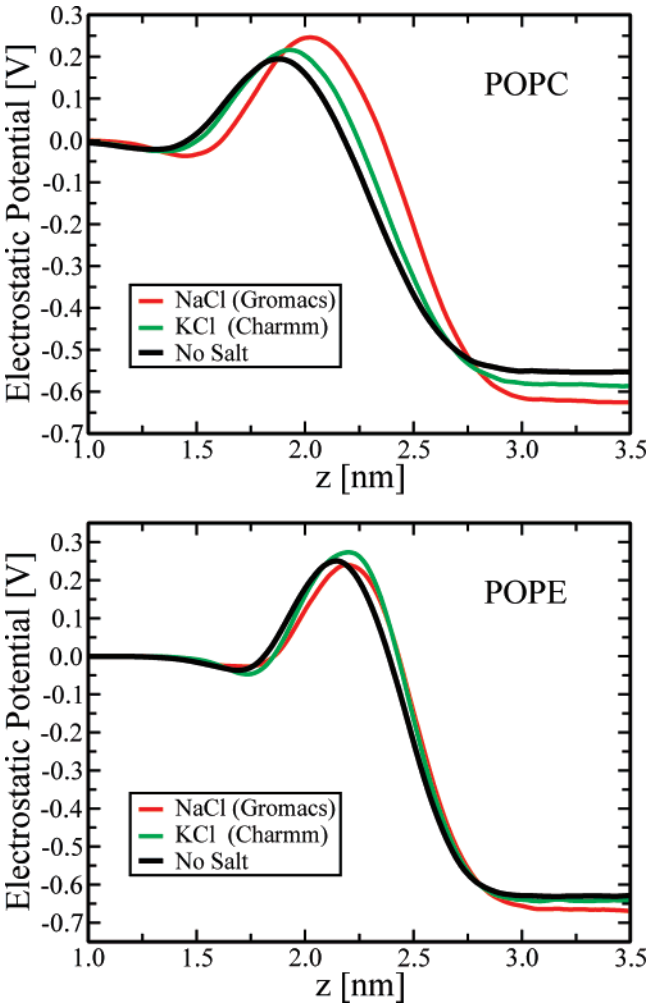

Figure 5. Electrostatic potential across a monolayer of POPC (top) and POPE (bottom) membranes; the potential is set to be zero at the membrane center ($z = 0$). Shown are representative results for the bilayer systems with NaCl and KCl as well as for salt-free systems.

weaker binding of K^+ ions to phospholipid membranes is also in line with the reported experimental[5,9] and computational[23] observations.

All distinct features observed in the mass density profiles for POPC membranes with NaCl and KCl are also translated to the distribution of partial charges in the systems (data not shown). The latter is crucial for membrane electrostatic properties such as the electrostatic potential across a membrane. For all considered POPC bilayers we computed the electrostatic potential from the Poisson equation by twice integrating over charge densities, see Figure 5 (top). For a salt-free POPC membrane we found that the overall potential difference between the membrane center and the aqueous phase is ~0.55 V. This value is in agreement with numerous computational studies,[6,12,15,21,27,47,48] while corresponding experimental values are in the range of 200−600 mV.[49−53] Addition of NaCl leads to a pronounced change in the electrostatic potential of a PC membrane: The peak of the potential in the region of the lipid−water interface increases and is shifted toward the water phase, reflecting most likely a considerable reorientation of head group dipoles. The overall potential difference across a leaflet increases to 0.63 V, see Figure 5 (top). This effect was also observed in previous MD simulation studies.[6,12,15] Remarkably, it was found to be almost insensitive to the force-field employed for ions. In turn, the effect of KCl on the electrostatic properties of POPC membranes is much weaker, in agreement with the weaker binding of K^+ ions reported above. When the Charmm force field was employed for ions, one observed only slight changes in the electrostatic potential, the increase of the potential across a monolayer being just 0.04 V as compared to a salt-free bilayer (Figure 5 (top)). For Gromacs simulations we did not observe any influence of KCl on the electrostatic potential (data not shown).

B. Effect of Monovalent Salt on POPE Membranes. Now we turn to the discussion of the effects of monovalent salt on the properties of PE membranes. The main difference between PC and PE lipids lies in the nature of their head groups, see Figure 1. POPE has a primary amine in its head group (instead of a choline moiety in POPC), for which reason POPE lipids are capable for the formation of both intra- and intermolecular hydrogen bonds.[54] As a result, the water−lipid interface of a POPE membrane is considerably more densely packed as compared to that of a POPC membrane. This inevitably should hinder the binding of ions and reduce salt effects overall.

Salt-Free POPE. For the area per lipid of a salt-free POPE bilayer, we found the value of 0.519 nm^2, see Table 2. This value is in very good agreement with reported MD studies of unsaturated PE membranes under similar conditions.[42,43,55] The experimental data for phospholipid bilayers can scatter consider-

ably (as much as 10−15% as shown for dipalmitoylphosphatidylcholine, DPPC).[56] A value of 0.56 nm^2 was reported for the area per lipid for a POPE bilayer,[57] which is somewhat larger than the area found in our study. Overall, it has been proposed that most up-to-date force-fields available for PE lipids underestimate the area per lipid,[58] but the difference seems to be less than four percent and hence reasonable. Furthermore, in recent studies where the present POPE force-field was employed for modeling asymmetric PC/PE membranes, one found good agreement with experimental results.[27] Strong hydrogen bonding between PE head groups also leads to a considerable difference in the orientation of head group dipoles as compared to PC bilayers: The average angle between the P−N vector and the outward bilayer normal for a POPE membrane is ∼93 degrees, i.e., PE head group dipoles on average point slightly to the membrane interior. The lateral diffusion coefficient D_L of a salt-free POPE membrane was found to be $D_L = (1.16 \pm 0.30) \times 10^{-8}$ cm^2/s, see Table 3. This value is close to the range of lateral diffusion rates $(2-4) \times 10^{-8}$ cm^2/s reported in a recent computational study[59] for a stearoyloleoylphosphatidylethanolamine (SOPE) bilayer. However, it is considerably lower than $D_L = (8 \pm 1) \times 10^{-8}$ cm^2/s measured for POPE lipids at $T = 306$ K by NMR techniques.[60] In part, this can be associated with the fact that the force-field employed for a POPE lipid bilayer underestimates the area per lipid. Furthermore, we would like to stress that any computational estimates for the POPE diffusion coefficient should be taken with caution: a POPE membrane is a much more densely packed structure compared to its POPC counterpart, which implies that finding a statistically reasonable evaluation for D_L should be based on trajectories much longer than 100 ns presented here.

POPE Under the Influence of NaCl. When NaCl salt is added, one can observe binding of sodium ions to a POPE membrane, the binding being much weaker compared to POPC membranes, see Table 2. This can also be seen in Figure 6 (top), where we have presented the time evolution of coordination numbers N_C of sodium ions with lipid carbonyl and water oxygens (since the behavior of N_C was found to be essentially similar in simulations with Gromacs and Charmm parameters for Na^+ ions, we chose to present results for the Charmm force-field only). The binding of a Na^+ ion has almost no effect on the area per lipid, which can be explained by the fact that a POPE bilayer without salt already represents a rather densely packed structure due to substantial hydrogen bonding. As seen from Table 3, the lateral diffusion coefficients demonstrate some decrease under the presence of NaCl; however, large error margins (20−25%) make it difficult to draw a definitive conclusion. The overall fraction of bound sodium ions in the POPE bilayer system is found to be much smaller than in the case of a POPC bilayer, namely with Gromacs parameters one finds 0.24 for POPE bilayers versus 0.87 for POPC bilayers; in simulations with Charmm parameters a somewhat larger value of 0.34 is observed for POPE bilayers, which is perhaps due to the smaller size of Na^+ ions in the Charmm force field. However, the binding of adsorbed Na^+ ions to lipid carbonyl oxygens is stronger when the Gromacs force field is employed for ions; in this case a Na^+ ion binds on average to ∼3 PE lipids, while for Charmm we observe $\langle N_{coord}^{(cations)} \rangle \simeq 2.38$, see Table 2. The stronger binding of Na^+ ions with Gromacs parameters can also be seen by inspecting the component-wise density profiles presented in Figure 7 (left column): The peak of the density for sodium ions with Gromacs parameters coincides with the peak corresponding to POPE carbonyl oxygens, while it is shifted to the water phase and even develops a small second peak close to the interface when the Charmm force-field is employed for ions. In particular, this leads to a somewhat stronger reorientation of P−N dipoles toward the aqueous phase in Charmm simulations, see Table 2.

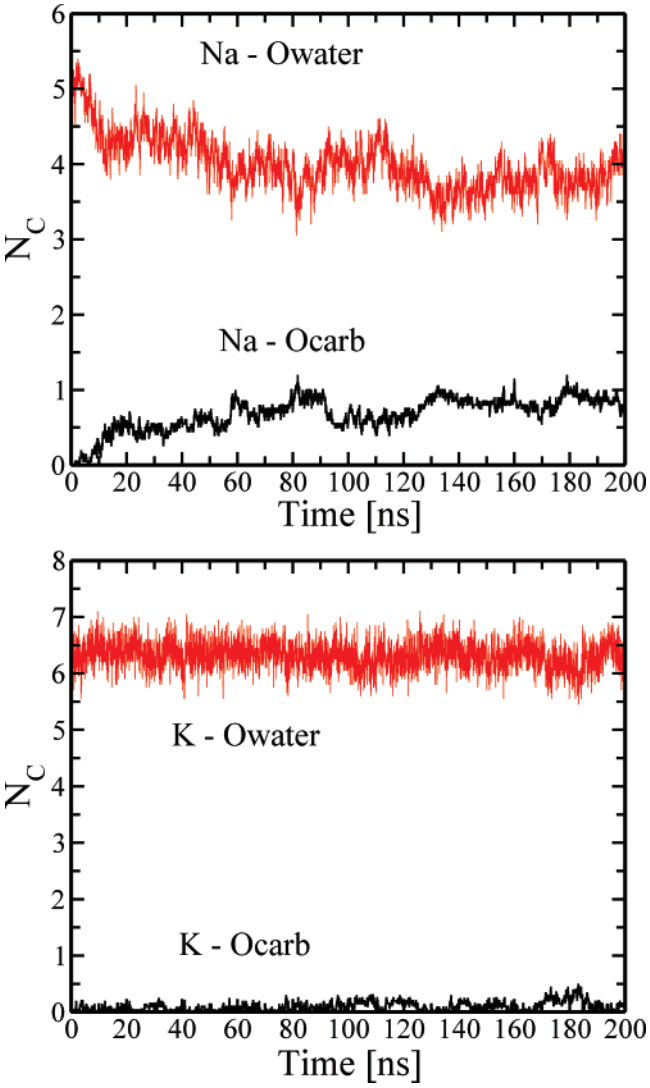

Figure 6. Time evolution of coordination numbers N_C of sodium (top) and potassium (bottom) ions with lipid carbonyl and water oxygens for POPE membranes. Shown are results for Charmm force-field parameters employed for ions.

As PE head groups are capable for hydrogen bonding, we performed a thorough analysis of intra- and intermolecular hydrogen bonds (H-bonds) for all simulated POPE bilayers, see Table 4. Following ref 55, a hydrogen bond was considered to exist if the distance between the acceptor and the NH_3 hydrogen was smaller than 0.25 nm and the angle "donor-H-acceptor" exceeded 60 degrees. For a salt-free POPE bilayer the average number of intramolecular H-bonds was found to be ∼1.33, the majority of them being provided by H-bonds with the 1Ophos atom (the average length of the corresponding hydrogen bond on the 1Ophos atom is found to be 0.2 nm, whereas the donor−acceptor distance equals 0.49 nm as extracted from the radial distribution function) and, to a considerably lesser extent, with the 2Ocarb atom, see Table 4 and Figure 1 for the labeling of lipid oxygen atoms. The overall number of intramolecular hydrogen bonds is in good agreement with the value of 1.32 reported in a recent simulation study[58] for a dipalmitoylphosphatidylethanolamine, DPPE, which employed a similar force-field.

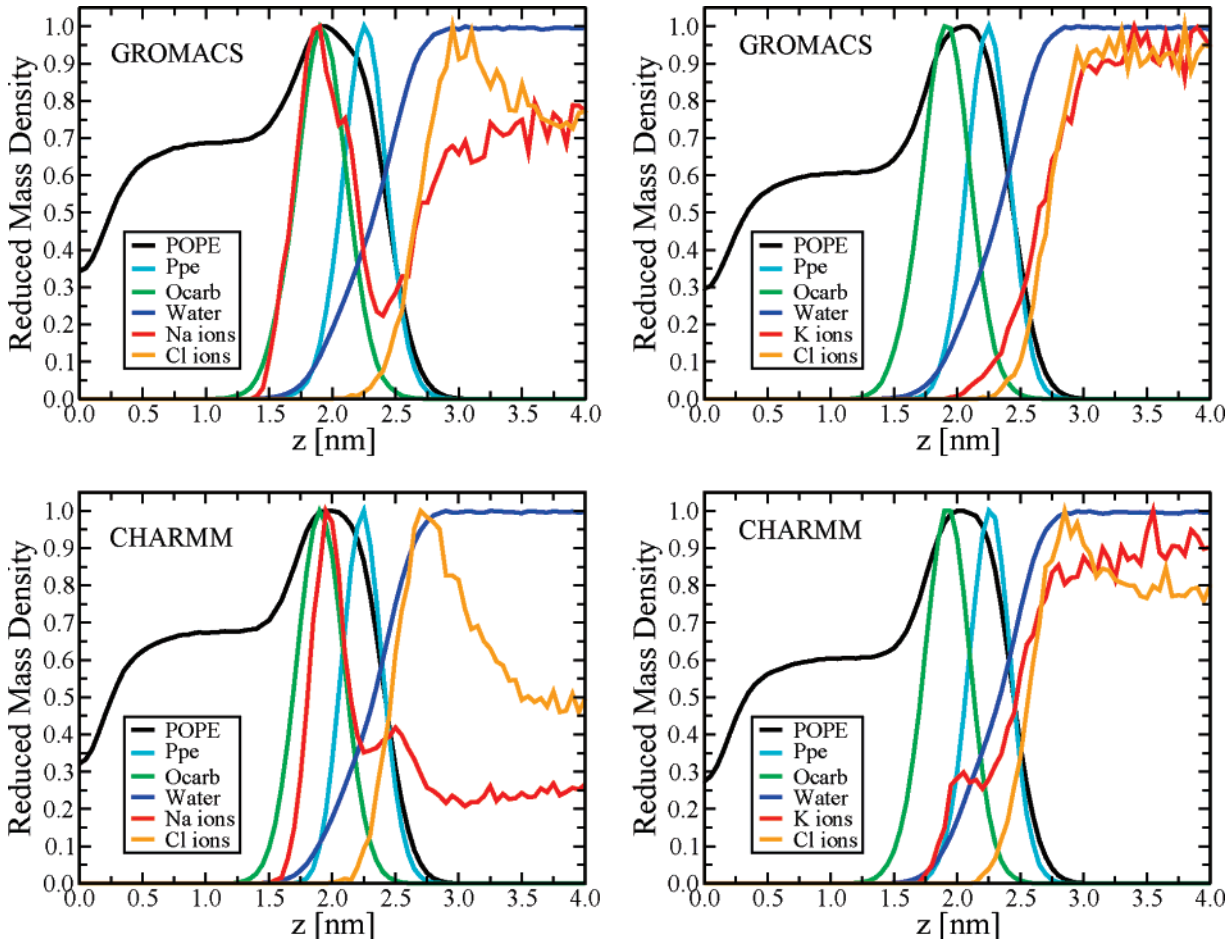

Figure 7. Component-wise density profiles (reduced by the maximal value of each component) as a function of the distance z from the bilayer center ($z = 0$). Shown are results for POPE bilayers with NaCl (left) and KCl (right), salt ions being described by Gromacs (top) and Charmm (bottom) force-fields. All density profiles were averaged over two leaflets.

TABLE 4: Hydrogen Bonding for POPE Membranes with Monovalent Salt

	POPE		POPE + NaCl[a]		POPE + KCl[a]	
atom	intra	inter	intra	inter	intra	inter
1Ophos	1.111	0.005	1.106 (1.103)	0.006 (0.003)	1.111 (1.109)	0.003 (0.004)
2Ophos	0.0003	0.306	0.0002 (0.0002)	0.299 (0.306)	0.0002 (0.0003)	0.275 (0.304)
3Ophos	0.0004	0.328	0.0005 (0.0003)	0.328 (0.342)	0.0005 (0.0004)	0.360 (0.373)
4Ophos	0.004	0.021	0.004 (0.005)	0.020 (0.019)	0.005 (0.005)	0.020 (0.017)
2Ocarb	0.179	0.343	0.158 (0.129)	0.289 (0.351)	0.154 (0.172)	0.354 (0.349)
1Ocarb	0.022	0.135	0.012 (0.015)	0.142 (0.135)	0.021 (0.016)	0.156 (0.147)
Total	1.33 ± 0.01	1.15 ± 0.01	1.29 (1.26)	1.10 (1.18)	1.30 (1.30)	1.19 (1.22)
Owater	0.99 ± 0.02		1.08 (1.01)		0.99 (0.93)	

[a] Presented are values for the simulations in which the Gromacs force-field was employed for ions (corresponding values for simulations with Charmm parameters are shown in brackets).

We note that this value has to be taken with caution as it is rather sensitive to the definition of the hydrogen bond. In a recent simulation study of mixed phosphatidylethanolamine/phosphatidylglycerol bilayers Murzyn et al.[61] reported the value of 0.22 for the overall number of intra-PE bonds. In their study the hydrogen bond was considered to be formed when the donor and acceptor are closer than 0.325 nm and the acceptor−donor-hydrogen angle is smaller than 35 degrees.[61] We recall that in our case the average donor−acceptor distance is 0.49 nm, so that the use of the criterion by Murzyn et al. should lead to considerably smaller values of intramolecular bonds compared to 1.33 reported above. Indeed, using the definition of the hydrogen bond from ref 61, we ended up with just 0.12 intramolecular bonds for PE lipids. Furthermore, we found that PE forms on average 1.15 intermolecular H-bonds in line with previous computational studies,[55] the main sites for H-bonds being 2Ophos, 3Ophos, 2Ocarb, and 1Ocarb atoms.

The presence of NaCl has some effect on hydrogen bonding. Binding of Na^+ ions to lipid carbonyl oxygens is able to break H-bonds associated with them. In particular, such a breakage leads to drop in the overall number of intramolecular H-bonds as observed from Table 4. As far as intermolecular H-bonding is concerned, the effect of NaCl is found to depend on the choice of the force-field for ions. The strong interlipid binding of Na^+ ions observed with Gromacs parameters results in a notable breaking of intermolecular H-bonds, so that we observe a drop in the total number of H-bonds of this type. Furthermore, the reorientation of head group dipoles toward the aqueous phase makes NH_3 groups more exposed to water molecules, increasing their hydration. In contrast, the weaker binding of sodium ions

seen in simulations with Charmm ion parameters does not break interlipid H-bonds which involve Ocarb atoms, and since the binding brings lipids closer, one observes a slight increase in the overall number of intermolecular H-bonds through enhancement of H-bonds associated with phosphate groups, see Table 4. The level of hydration stays almost unchanged, because an increased exposure of NH_3 groups to water due to head group reorientation is compensated by an increase in the number of intermolecular H-bonds.

POPE Under the Influence of KCl. As far as KCl salt is concerned, its influence on POPE membranes can be characterized as very weak or even negligible. We find that potassium ions do not bind to the lipid−water interface; this feature is observed consistently for both sets of force-field parameters for ions. In simulations with Gromacs parameters the average number of adsorbed ions is essentially zero, while in Charmm runs one has $\langle \chi_{\text{bound}}^{(\text{cations})} \rangle \simeq 0.06$, i.e., approximately 1 bound potassium ion out of 20, see Table 2. Figure 6 (bottom) further illustrates the very weak binding of potassium ions for the latter system. Therefore, almost all K^+ ions are located in the aqueous phase and not in the membrane-water interface; only a tiny peak is observed in the potassium density profile inside the interface between carbonyl oxygens and phosphate groups, see Figure 7 (right) illustrating this for simulations with Charmm parameters. The presence of a large amount of potassium ions in the water phase may be the reason why PE head groups are oriented more toward the interior of the membrane as compared to a salt-free system (Table 2): K^+ ions likely push NH_3 further out of the water phase. The above change in the average head group tilt seems to be responsible for the slight increase in the total number of intermolecular H-bonds in the presence of KCl salt, see Table 4, and for a drop in the hydration of NH_3 groups seen with Charmm parameters. As far as the lateral diffusion is concerned, we found a surprising drop in the diffusion coefficients, see Table 3, despite of the lack of ion binding to the lipid−water interface. Because of the large statistical errors, it is, however, unclear whether there are physical grounds behind this effect or is it simply due to insufficient sampling.

We conclude this section by considering the electrostatic properties of the membranes. As emphasized above, monovalent cations such as Na^+ ions bind to POPE membranes to a significantly lesser extent than in POPC bilayers, whereas K^+ ions do not adsorb on the membrane surface at all. As a consequence, the average dipole moment of PE head groups does not change significantly through reorientation of the head group dipoles. Therefore, one should not expect a pronounced impact of monovalent salt on the electrostatic properties of POPE membranes. Indeed, as is seen from the electrostatic potential across a PE monolayer presented in Figure 5 (bottom), the membrane potential is hardly affected by the presence of monovalent salt at all.

IV. Summary and Conclusions

Plasma membranes of eukaryotic cells are characterized by a distinctly different lipid distribution in the extracellular (outer) and cytosolic (inner) sides of the membrane. The outer leaflet is mainly comprised of PCs, whereas the main component of the inner leaflet is PE. Under physiological conditions, these leaflets interact with an aqueous salt solution whose composition is also specific to the monolayer in question: PCs are influenced by monovalent NaCl, whereas PEs, in turn, are under the influence of KCl. The biological relevance of these salts and their significance on cell membrane behavior have been realized in many contexts, but the details of their interplay, and especially the differences arising from the specific ion−lipid interactions, have largely remained unclear. In this study, we have used extensive atomic-scale molecular dynamics simulations to shed light on these issues. To the best of our knowledge, the present work is the first simulation study which explores the effects of monovalent salt on PE bilayers.

We have demonstrated that the effects of monovalent salt on a phospholipid membrane are mainly determined by the binding of cations to the lipid−water interface: Cations penetrate rather deep into the interface, bind to the carbonyl region of lipid molecules, and form rather stable complexes with lipids, whereas chloride anions mostly stay in the water phase nearby the membrane surface. Importantly, all the simulations were performed with two different sets of parameters for salt ions (implemented in Gromacs and Charmm force-fields), providing a solid basis for our conclusions.

The strength and character of the cation−lipid interactions have been found to be quite different for the different types of lipids and cations. The strongest interactions have been observed for PC membranes with sodium cations. The tight binding of Na^+ ions to PC lipid bilayers leads to a notable decrease in the area per lipid accompanied by a more vertical orientation of PC head groups with respect to the membrane surface, by a considerable slowing down of the lateral lipid mobility, and by an increase in the potential difference across a monolayer. These findings are found to be robust to a choice of force-field parameters employed for ions. As for potassium ions, their binding to PC membranes and, therefore, the overall salt induced effects are found to be much weaker compared to Na^+. This is mostly due to the larger size of a K^+ ion, which implies a smaller ionic surface charge and a less ordered first hydration shell. The weaker role of potassium ions compared to Na^+ was observed consistently with all force field parametrizations we considered. Nevertheless, there is reason to mention that while K^+ ions bind (weakly) to the carbonyl region of a PC membrane when the Charmm force-field is employed for ions, such a binding is not observed when one employed the Gromacs force-field, which seems to exaggerate the size of a potassium ion.

Considering PE membranes, the effects of NaCl and KCl salts on the bilayers were found to be much weaker than in the case of PC membranes. This is a direct consequence of the different nature of PC and PE head groups. More specifically, PE has a primary amine in its head group, making it capable for the formation of both intra- and intermolecular hydrogen bonds. This gives rise to a considerably more densely packed lipid−water interface compared to the case of a PC membrane, and inevitably hinders the binding of ions, reducing salt effects overall. Meanwhile, KCl in particular is found to have a negligible effect on PE lipid membranes as potassium ions do not bind to the PE lipid−water interface. These conclusions are supported by both force fields we have considered for ions. As expected, however, the quantitative features depend to some extent on the details of the force-field parametrization. Above all, the binding of Na^+ ions is somewhat stronger when the Gromacs parameters are employed, leading to a substitution of some intermolecular hydrogen bonds by ionic bridges.

Our findings are in line with the available experimental[6−9] and computational studies[6,12,15,23] and provide further insight into the effects of monovalent salt on cell membranes. Importantly, since potassium ions are the main monovalent cations in the intracellular fluid, their negligible influence on PE bilayers suggests that salt has no strong impact on PE-rich lipid domains in the inner leaflet of cell membranes. Meanwhile, sodium ions, being the major ionic species in the extracellular fluid, bind

tightly to the carbonyl region of PC bilayers and change lipid packing to a significant extent. Therefore, one may expect that monovalent salt, affecting lipid domains in the outer leaflet but not in the inner leaflet is able to decrease the difference in packing properties of lipid domains on the two sides of (plasma) cell membranes.

Acknowledgment. Funding from the Academy of Finland (I.V.) is gratefully acknowledged. The simulations were performed at the Finnish IT Center for Science and on the HorseShoe (DCSC) supercluster at the University of Southern Denmark.

References and Notes

(1) Gennis, R. B. *Biomembranes: Molecular Structure and Function;* Springer-Verlag: New York, 1989.
(2) Zachowski, A. *Biochem. J.* **1993**, *294*, 1−14.
(3) Altenbach, C.; Seelig, J. *Biochemistry* **1984**, *23*, 3913−3920.
(4) Herbette, L.; Napolitano, C. A.; McDaniel, R. V. *Biophys. J.* **1984**, *46*, 677−685.
(5) Binder, H.; Zschörnig, O. *Chem. Phys. Lipids* **2002**, *115*, 39−61.
(6) Böckmann, R. A.; Hac, A.; Heimburg, T.; Grubmüller, H. *Biophys. J.* **2003**, *85*, 1647−1655.
(7) Garcia-Manyes, S.; Oncins, G.; Sanz, F. *Biophys. J.* **2005**, *89*, 1812−1826.
(8) Garcia-Manyes, S.; Oncins, G.; Sanz, F. *Electrochim. Acta* **2006**, *51*, 5029−5036.
(9) Fukuma, T.; Higgins, M. J.; Jarvis, S. P. *Phys. Rev. Lett.* **2007**, *98*, 106101.
(10) Niemela, P.; Ollila, S.; Hyvonen, M. T.; Karttunen, M.; Vattulainen, I. *PLoS Comput. Biol.* **2007**, *3*, 304−312.
(11) Böckmann, R. A.; Grubmüller, H. *Angew. Chem. Int. Ed.* **2004**, *43*, 1021−1024.
(12) Pandit, S. A.; Bostick, D.; Berkowitz, M. L. *Biophys. J.* **2003**, *84*, 3743−3750.
(13) Sachs, J.; Woolf, T. B. *J. Am. Chem. Soc.* **2003**, *125*, 8742−8743.
(14) Sachs, J. N.; Nanda, H.; Petrache, H. I.; Woolf, T. B. *Biophys. J.* **2004**, *86*, 3772−3782.
(15) Gurtovenko, A. A. *J. Chem. Phys.* **2005**, *122*, 244902.
(16) Gurtovenko, A. A.; Vattulainen, I. *J. Am. Chem. Soc.* **2005**, *127*, 17570−17571.
(17) Pandit, S. A.; Berkowitz, M. L. *Biophys. J.* **2002**, *82*, 1818−1827.
(18) Pandit, S. A.; Bostick, D.; Berkowitz, M. L. *Biophys. J.* **2003**, *85*, 3120−3131.
(19) Mukhopadhyay, P.; Monticelli, L.; Tieleman, D. P. *Biophys. J.* **2004**, *86*, 1601−1609.
(20) Pedersen, U. R.; Leidy, C.; Westh, P.; Peters, G. H. *Biochim. Biophys. Acta* **2006**, *1758*, 573−582.
(21) Gurtovenko, A. A.; Patra, M.; Karttunen, M.; Vattulainen, I. *Biophys. J.* **2004**, *86*, 3461−3472.
(22) Gurtovenko, A. A.; Miettinen, M.; Karttunen, M.; Vattulainen, I. *J. Phys. Chem. B* **2005**, *109*, 21126−21134.
(23) Gurtovenko, A. A.; Vattulainen, I. *Biophys. J.* **2007**, *92*, 1878−1890.
(24) Patra, M.; Karttunen, M. *J. Comput. Chem.* **2004**, *25*, 678−689.
(25) Berger, O.; Edholm, O.; Jahnig, F. *Biophys. J.* **1997**, *72*, 2002−2013.
(26) Tieleman, D. P.; Berendsen, H. J. C. *Biophys. J.* **1998**, *74*, 2786−2801.
(27) Gurtovenko, A. A.; Vattulainen, I. *J. Am. Chem. Soc.* **2007**, *129*, 5358−5359.
(28) Berendsen, H. J. C.; Postma, J. P. M.; van Gunsteren, W. F.; Hermans, J. In *Intermolecular Forces;* Pullman, B., Ed.; Reidel: Dordrecht, 1981; pp 331−342.
(29) Straatsma, T. P.; Berendsen, H. J. C. *J. Chem. Phys.* **1988**, *89*, 5876−5886.
(30) Lindahl, E.; Hess, B.; van der Spoel, D. *J. Mol. Model.* **2001**, *7*, 306−317.
(31) Beglov, D.; Roux, B. *J. Chem. Phys.* **1994**, *100*, 9050−9063.
(32) Darden, T.; York, D.; Pedersen, L. *J. Chem. Phys.* **1993**, *98*, 10089−10092.
(33) Essmann, U.; Perera, L.; Berkowitz, M. L.; Darden, T.; Lee, H.; Pedersen, L. G. *J. Chem. Phys.* **1995**, *103*, 8577−8592.
(34) Patra, M.; Karttunen, M.; Hyovnen, M. T.; Falck, E.; Lindqvist, P.; Vattulainen, I. *Biophys. J.* **2003**, *84*, 3636−3645.
(35) Patra, M.; Karttunen, M.; Hyovnen, M. T.; Falck, E.; Vattulainen, I. *J. Phys. Chem. B* **2004**, *108*, 4485−4494.
(36) Patra, M.; Hyvonen, M. T.; Falck, E.; Sabouri-Ghomi, M.; Vattulainen, I.; Karttunen, M. *Comput. Phys. Commun.* **2007**, *176*, 14−22.
(37) Berendsen, H. J. C.; Postma, J. P. M.; van Gunsteren, W. F.; DiNola, A.; Haak, J. R. *J. Chem. Phys.* **1984**, *81*, 3684−3690.
(38) Hyslop, P. A.; Morel, B.; Sauerheber, R. D. *Biochemistry* **1990**, *29*, 1025−1038.
(39) Lantzsch, G.; Binder, H.; Heerklotz, H.; Wendling, M.; Klose, G. *Biophys. Chem.* **1996**, *58*, 289−302.
(40) König, B.; Dietrich, U.; Klose, G. *Langmuir* **1997**, *13*, 525−532.
(41) Smaby, J. M.; Momsen, M. M.; Brockman, H. L.; Brown, R. E. *Biophys. J.* **1997**, *73*, 1492−1505.
(42) Mukhopadhyay, P.; Vogel, H. J.; Tieleman, D. P. *Biophys. J.* **2004**, *86*, 337−345.
(43) Leekumjorn, S.; Sum, A. K. *J. Phys. Chem. B.* **2007**, *111*, 6026−6033.
(44) Dzubiella, J.; Hansen, J.-P. *J. Chem. Phys.* **2005**, *122*, 234706.
(45) Aqvist, J. *J. Phys. Chem.* **1990**, *94*, 8021−8024.
(46) Shrivastava, I. H.; Tieleman, D. P.; Biggind, P. C.; Sansom, M. S. P. *Biophys. J.* **2002**, *83*, 633−645.
(47) Chiu, S. W.; Clark, M.; Balaji, V.; Subramaniam, S.; Scott, H. L.; Jacobsson, E. *Biophys. J.* **1995**, *69*, 1230−1245.
(48) Smondyrev, A. M.; Berkowitz, M. L. *J. Chem. Phys.* **1999**, *111*, 9864−9870.
(49) Hladky, S. B.; Haydon, D. A. *Biochim. Biophys. Acta* **1973**, *318*, 464−468.
(50) Pickard, A. D.; Benz, R. *J. Membr. Biol.* **1978**, *44*, 353−376.
(51) Flewelling, R. F.; Hubbel, W. L. *Biophys. J.* **1986**, *49*, 541−552.
(52) Gawrisch, K.; Ruston, D.; Zimmerberg, J.; Parsegian, V. A.; Rand, R. P.; Fuller, N. *Biophys. J.* **1992**, *61*, 1213−1223.
(53) Clarke, R. J. *Adv. Colloid Interface Sci.* **2001**, *89*, 263−281.
(54) McIntosh, T. J. *Chem. Phys. Lipids* **1996**, *81*, 117−131.
(55) de Vries, A. H.; Mark, A. E.; Marrink, S. J. *J. Phys. Chem. B* **2004**, *108*, 2454−2463.
(56) Nagle, J. F.; Tristram-Nagle, S. *Biochim. Biophys. Acta* **2000**, *1469*, 159−195.
(57) Rand, R. P.; Parsegian, V. A. *Biochim. Biophys. Acta* **1989**, *988*, 351−376.
(58) Leekumjorn, S.; Sum, A. K. *Biophys. J.* **2006**, *90*, 3951−3965.
(59) Pitman, M. C.; Suits, F.; Gawrisch, K.; Feller, S. E. *J. Chem. Phys.* **2005**, *122*, 244715.
(60) Polozov, I. V.; Gawrisch, K. *Biophys. J.* **2004**, *87*, 1741−1751.
(61) Murzyn, K.; Róg, T.; Pasenkiewicz-Gierula, M. *Biophys. J.* **2005**, *88*, 1091−1103.